Available online at www.sciencedirect.com
ScienceDirect
Journal of Theoretical Biology 249 (2007) 384–394
Journal of Theoretical Biology
www.elsevier.com/locate/yjtbi

T cell development in the thymus: From periodic seeding to constant output

Anna Q. Cai[a], Kerry A. Landman[a,*], Barry D. Hughes[a], Colleen M. Witt[b]

[a]*Department of Mathematics and Statistics, The University of Melbourne, Vic. 3010 Australia*
[b]*RCMI Advanced Imaging Center, Department of Biology, University of Texas at San Antonio, TX 78249, USA*

Received 15 May 2007; received in revised form 27 July 2007; accepted 27 July 2007
Available online 9 August 2007

Abstract

T cell development occurs in the thymus throughout life. Recent experimental findings show that the seeding of the thymus by multipotent stem cells from the bone marrow is periodic rather than continuous, as previously assumed. However it is well known that the output rate of cells from the thymus is relatively constant. A quantitative model is used to verify the current hypotheses regarding T cell development in the steady state mouse thymus. The results show that the thymus could be at a periodic steady state with out-of-phase thymocyte populations. Experiments to examine possible periodic fluctuations in the thymus are proposed and methods for further analysis are outlined.

Keywords: Thymocytes; Thymus; Proliferation; Differentiation; Periodic oscillations

1. Introduction

T cell development begins with multipotent precursor stem cells being periodically released from the bone marrow and migrating into the thymus, where they undergo proliferation and differentiation before migrating out of the thymus as mature T cells. The murine thymus is made up of two lobes, each of which is compartmentalised into an outer cortex and inner medulla region. Development of T cells coincides with the tightly regulated movement of defined intermediate populations between these two major compartments (Witt and Robey, 2005). Fig. 1 is a photograph of an adult murine thymus with one such cortex and medulla region labelled.

The developmental program of T cells is summarised schematically in Fig. 2. Precursors to the T cell lineage are released periodically from the bone marrow, enter the bloodstream, and find their way to the thymus. Precursors enter at the cortico-medullary junction (CMJ) and fill up the finite number of niches available. The niches are found to be receptive to precursor cell seeding at periodic intervals, with the seeding cycle remaining relatively constant throughout life (Donskoy et al., 2003; Foss et al., 2001; Goldschneider, 2006). Cells at this developmental stage are not yet committed to becoming cells of the T lineage, but retain multi-potentiality. As they lack expression of either the CD4 or CD8 surface molecule, they are referred to as double negative (DN) cells. The DN population consists of four early T cell sub-sets, DN1–DN4.

Following their arrival at the CMJ, DN1 cells undergo numerous rounds of cell division (Penit et al., 1995; Vasseur et al., 2001). As cell division ceases, this population migrates away from the CMJ and into the mid-cortex where they progress to the DN2 stage and become developmentally committed to the T cell lineage. Cells continue to migrate outwards until they arrive at the outer region of the cortex known as the sub-capsular zone (SCZ) (Lind et al., 2001). Approximately one third of these cells successfully pass through a critical developmental checkpoint (DN3 stage) leading to robust cell division (DN4 stage) (Penit et al., 1995). As this second burst of proliferative activity subsides, the cells begin to express

*Corresponding author. Tel.: +613 83446762; fax: +613 83444599.
E-mail address: k.landman@ms.unimelb.edu.au (K.A. Landman).

0022-5193/$ - see front matter
doi:10.1016/j.jtbi.2007.07.028

both the CD4 and CD8 co-receptors and are now known as double positive (DP) cells. DP cells withdraw from the cell division cycle and lose their proliferative ability (Petrie and Zúñiga-Pflücker, 2007). The cortex is dominated in number by DP cells. Through contact with the stromal cells in the cortex, a small percentage of DP cells pass successfully through a second critical checkpoint known as *positive selection*. These cells receive survival signals through the selection process that allow them to mature further to the final stage of development, the single positive (SP) stage. In addition, the nature of the signal determines the lineage fate of the developing thymocyte; depending on the interactions, expression of either the CD4 or the CD8 surface molecule shuts off leaving the cell fated to mature into one of two T cell sub-populations, cytotoxic CD8+ or helper CD4+ cells. The vast majority of DP cells do not become selected, and therefore, receive no such survival signals. These cells eventually die in the cortex in 3–5 days time.

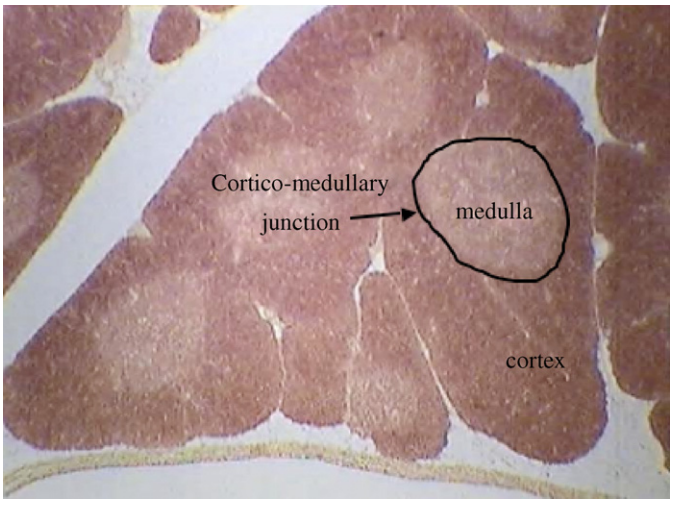

Fig. 1. A photograph of an adult mouse thymus with a cortex and medulla region labelled.

In contrast to all other sub-populations of developing T cells, positively selected DP thymocytes have access to the medulla. Experimental evidence shows that post-selected cells exhibit biased movement away from the thymic capsule and may be chemotactically attracted to the medulla (Witt et al., 2005a). Upon arrival in the medulla, SP cells interact with antigen presenting cells (APC) for their final test. APC present fragments of proteins

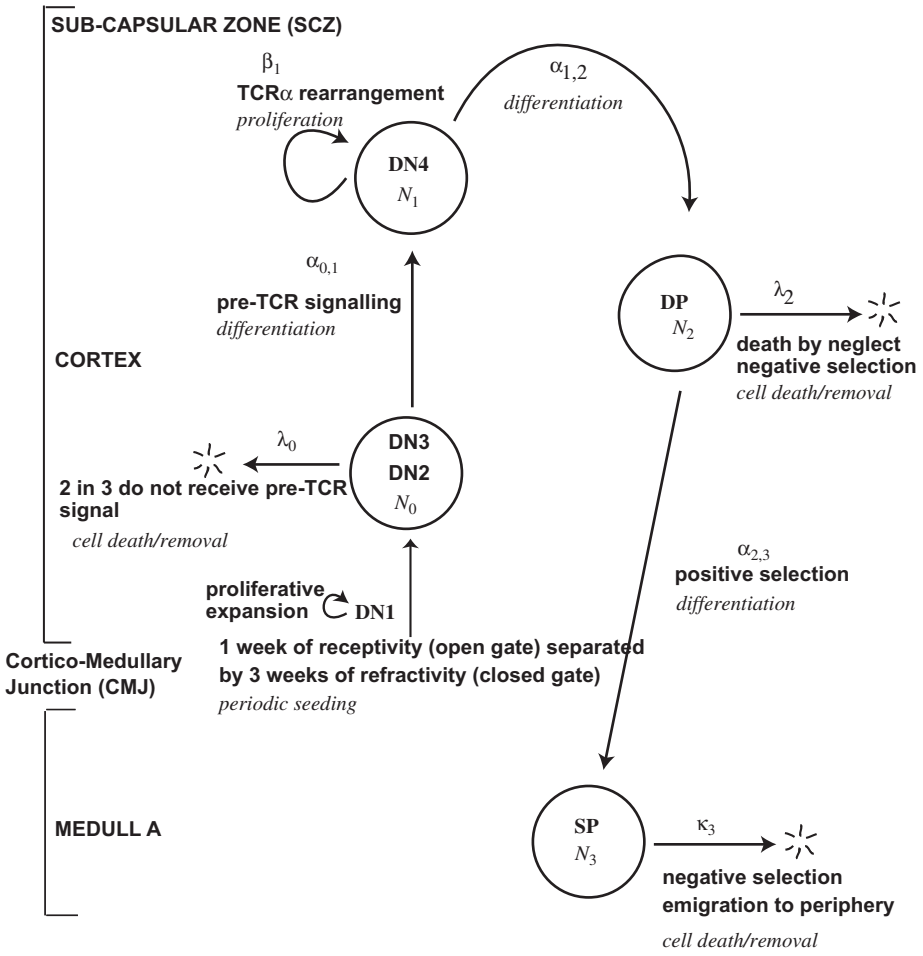

Fig. 2. A schematic diagram of T cell development in the thymus. In bold font are thymocyte populations and major developmental events. The modelled thymocyte populations and developmental events described by Eqs. (1)–(4) are in italic font.

produced by various host cells and tissues. These self-peptides are presented to the SP cell in the context of major histo-compatibility complexes (MHC) expressed on the surface of the APC. Thymocytes that react strongly to self-peptide MHC are deleted through a process known as *negative selection*. This is an important process which removes T cells that are likely to cause autoimmune reactions if they are released into the body. Mature T cells then emigrate from the thymus to the periphery where they are now fully equipped to execute their fated function.

We present a model of T cell development in the steady state murine thymus. During this time period, which commences at approximately 3–4 weeks of age, thymic maturation is complete and the thymus remains at a relatively fixed size for approximately 100 days and is producing T cells at a constant rate. After this time the onset of puberty causes the thymus to shrink gradually, a process termed involution. Shortman and co-workers, (Egerton et al., 1990; Shortman et al., 1990, 1991), measured the kinetics of thymocyte development from the double negative (DN) stage to the single positive (SP) stage using irradiated thymii reconstituted with donor cells. These experiments show that the differentiation process is sequential and has large fluctuations in cell number over the 26 days of experiment. Notably the number of thymocytes drops from 10^7 to 10^5 over 3 days during the transition between DP and SP stage. This demonstrates that only a small percentage of DP cells successfully receive positive selection signals. This size of fluctuation is normally unseen in the steady state thymus and is explained by the classical view that seeding of the thymus is continuous. However, recent experimental evidence using adoptive transfer of murine bone marrow into recipients by Foss et al. (2001) showed that progenitor cells seed the thymus in periodic waves of approximately 4 weeks, with one week of thymic receptivity separated by 3 weeks of refractivity. This seeding process is reviewed by Goldschneider (2006). These experiments were advantageous as they were performed in non-irradiated mice. In the time scale of the steady state thymus, the receptive seeding length (1 week) should be considered discrete. Thus, it is of interest to re-evaluate the steady state thymus with a quantitative description of the fluctuations in the thymocyte subpopulations and also to explain why T cell production appears constant.

Porritt et al. (2003) found that DN1 cells remain at the CMJ undifferentiated for 9–11 days after seeding and a sizeable portion remain at the CMJ for more than 2 weeks. Porritt et al. (2003) proposed that asynchronous release from the DN1 compartment can subsequently maintain later stage populations at constant levels. One interpretation of this claim is that control mechanisms operate independently of DN1 cells to release constant cell numbers in time. This appears unlikely as the percentage of donor DN1 population displays an exponential decay from 9 days post-transplant, which is more consistent with kinetics of constant rate (percentage) rather than constant cell number in time (Porritt et al., 2003; Fig. 1). Goldschneider (2006) also remarked in relation to data provided by Porritt et al. (2003) that by day 17 post-transplant the DN1 population would be completely depleted. An alternative synchronous development model, favored by Foss et al. (2001) and Goldschneider (2006) is that each wave of thymopoiesis occurs over two seeding periods and this temporal overlapping produces the appearance of relatively constant population composition of the thymus. The question of how T cell production appears constant can be best resolved using quantitative techniques rather than schematic arguments.

Mehr et al. (1995) first developed a model of thymocyte differentiation in the thymus using a system of nonlinear ordinary differential equations for the subsets DN, DP, and for both CD4 SP and CD8 SP. The growth and differentiation rates were found by searching the parameter space to produce the steady state composition of the thymus. Modified versions of this model have been used for investigating feedback regulation of development (Mehr et al., 1996) and for T cell development in humans (Ye and Kirschner, 2002). An extension of this model incorporating time delays during differentiation is provided in Shi and Ma (2006). The authors showed the equilibrium values are globally asymptotically stable for any time delay. Further analysis into the relationship between the time delays, the model parameter values, and the equilibrium values would be valuable to biologists. Wang and Krueger (2004) and Wang (2007) proposed an age-structured model and prescribed methods to find the age dependent growth nd differentiation fields of thymocytes in both the steady and pathological state of the thymus. Computer simulations of the entire thymus were carried out by Efroni et al. (2007). The models aforementioned did not take into account the periodic seeding of the thymus and assumed that the steady state thymus has a fixed composition of thymocyte populations. In this study, we take a discrete compartment approach, as in Mehr et al. (1995), to test the synchronous development hypothesis of Goldschneider and co-workers (Donskoy et al., 2003; Foss et al., 2001; Goldschneider, 2006). Based on our findings, we propose experiments that can examine the possible periodic oscillations in the steady state thymus.

2. The mathematical model

Following the completion of thymic maturation at 3–4 weeks of age, the thymus remains relatively constant in size, with a constant number of cells, until the onset of puberty. Here we present a model of thymocyte population kinetics of the steady state thymus.

The earliest progenitors, DN1 cells, remain undifferentiated at the CMJ for approximately 10 days where they undergo robust expansion. Following this proliferative burst, cells begin to move away from the CMJ where they differentiate through the DN2 and DN3 stages. Cell division at these developmental stages is negligible (Penit

et al., 1995). The total population of cells in the DN2 and DN3 stages is denoted by $N_0(t)$. We model the DN1 cells as the source term of N_0. A fraction of these cells then receive pre-TCR signalling and differentiate to the DN4 stage (also known as PreDP), modelled as $N_1(t)$. This population then undergoes cycling to produce the most numerically dominant population, the DP cells, modelled as $N_2(t)$. Finally, we let $N_3(t)$ be the population of SP cells, the most mature population. The units for N_0, N_1, N_2, and N_3, are cell number per thymus.

We assume linear kinetics and consider a general model,

$$\frac{dN_0}{dt} = \mathbf{Q}\sum_{n=0}^{\infty} S(t-nT) - \alpha_{0,1}N_0 - \lambda_0 N_0, \tag{1}$$

$$\frac{dN_1}{dt} = \alpha_{0,1}N_0 + \beta_1 N_1 - \alpha_{1,2}N_1, \tag{2}$$

$$\frac{dN_2}{dt} = \alpha_{1,2}N_1 - \alpha_{2,3}N_2 - \lambda_2 N_2, \tag{3}$$

$$\frac{dN_3}{dt} = \alpha_{2,3}N_2 - \kappa_3 N_3. \tag{4}$$

The developmental flow of the populations, as represented by the model equations (1)–(4), is illustrated in Fig. 2, where the actual thymocyte populations being modelled and the major developmental events are written in bold font. In Eq. (1), T is the seeding period, $\mathbf{Q}$ is the number of cells differentiating to N_0 per seeding period and $S(t)$ is a probability distribution such that

$$\int_0^T S(t)\,dt = 1. \tag{5}$$

The exact distribution of $S(t)$ has not been experimentally determined. We assume a normal distribution for $S(t)$ as an appropriate, simple choice. Most of a normal distribution is contained within six standard deviations. Thus, a criterion that $T > 6\sigma$, where σ is one standard deviation, would allow the overlaps between seedings to be negligible.

Maturation or differentiation rates between populations are denoted by $\alpha_{i,j}$ with the subscripts representing differentiation from i to j. Due to the combinatorial nature of gene arrangement, approximately one in three N_0 cells form a functional pre-TCR (T cell receptor) to receive signalling. We use a death/removal term λ_0 such that $\lambda_0 = 2\alpha_{0,1}$ to take into account this ratio. The only modelled population with significant proliferative ability is N_1 and its net rate of increase due to division and death/removal is denoted by β_1. It is assumed that $\beta_1 < \alpha_{1,2}$, otherwise the N_1 population would grow without bound. The majority of N_2 do not survive, primarily because they fail to pass positive selection, but also possibly due to some negative selection. This removal rate is collectively modelled by λ_2. The death/removal rate of N_3, κ_3, includes negative selection and emigration from the thymus.

We are interested in the asymptotic behaviour of the model which corresponds to the steady state thymus. The model is solved with initial conditions

$$N_i(0) = 0, \quad i = 0,1,2,3, \tag{6}$$

until it reaches steady state. We scale the densities by their respective mean steady state densities $\tilde{N}_0, \tilde{N}_1, \tilde{N}_2$, and $\tilde{N}_3$ and the time by the period T. We also introduce the scaled inflow rates of each population denoted by Q_i and the scaled outflow rates Q_i'.

$$N_0 = \tilde{N}_0\,\overline{N_0}, \quad N_1 = \tilde{N}_1\overline{N_1}, \quad N_2 = \tilde{N}_2\overline{N_2}, \quad N_3 = N_3\tilde{N}_3, \tag{7}$$

$$t = T\bar{t}, \quad \sigma = T\bar{\sigma}, \tag{8}$$

$$Q_0 = \frac{\mathbf{Q}}{\tilde{N}_0}, \quad Q_0' = T(\alpha_{0,1} + \lambda_0), \tag{9}$$

$$Q_1 = \frac{T\alpha_{0,1}\tilde{N}_0}{\tilde{N}_1}, \quad Q_1' = T(\alpha_{1,2} - \beta_1), \tag{10}$$

$$Q_2 = \frac{T\alpha_{1,2}\tilde{N}_1}{\tilde{N}_2}, \quad Q_2' = T(\alpha_{2,3} + \lambda_2), \tag{11}$$

$$Q_3 = \frac{T\alpha_{2,3}\tilde{N}_2}{\tilde{N}_3}, \quad Q_3' = T\kappa_3. \tag{12}$$

We consider the scaled source function defined as

$$\overline{S}(\bar{t}) = TS(t). \tag{13}$$

The bar notation is dropped from here on for brevity.

The general properties of the model are analysed by replacing the source function $S(t)$ with a one-sided delta function $\delta_+(t)$, which is governed by

$$\int_{0^+}^{\infty} \delta_+(t)\,dt = 1. \tag{14}$$

Hence we consider the Green functions of the model denoted by G_0, G_1, G_2, G_3. The relationship between the general solution and the Green functions is

$$N_i(t) = \int_0^t G_i(t-t')S(t')\,dt', \quad i = 0,1,2,3. \tag{15}$$

The equations governing the Green functions are

$$\frac{dG_0}{dt} = Q_0\sum_{n=0}^{\infty}\delta_+(t-n) - Q_0'G_0, \tag{16}$$

$$\frac{dG_1}{dt} = Q_1G_0 - Q_1'G_1, \tag{17}$$

$$\frac{dG_2}{dt} = Q_2G_1 - Q_2'G_2, \tag{18}$$

$$\frac{dG_3}{dt} = Q_3G_2 - Q_3'G_3. \tag{19}$$

The solutions to the system Eqs. (16)–(19) for the general case where the scaled outflow rates of each population are

unequal (that is $Q'_0 \neq Q'_1$, $Q'_0 \neq Q'_2$, etc.) are

$$G_0 = \sum_{n=0}^{\infty} H(t-n) Q_0 e^{-Q'_0(t-n)}, \tag{20}$$

$$G_1 = \sum_{n=0}^{\infty} H(t-n) \frac{Q_0 Q_1}{Q'_0 - Q'_1} \{e^{-Q'_1(t-n)} - e^{-Q'_0(t-n)}\}, \tag{21}$$

$$G_2 = \sum_{n=0}^{\infty} H(t-n) \frac{Q_0 Q_1 Q_2}{Q'_0 - Q'_1} \times \left(\frac{1}{Q'_1 - Q'_2} \{e^{-Q'_2(t-n)} - e^{-Q'_1(t-n)}\} \right. \tag{22}$$

$$\left. - \frac{1}{Q'_0 - Q'_2} \{e^{-Q'_2(t-n)} - e^{-Q'_0(t-n)}\} \right), \tag{23}$$

$$G_3 = \sum_{n=0}^{\infty} H(t-n) \frac{Q_0 Q_1 Q_2 Q_3}{(Q'_1 - Q'_2)(Q'_0 - Q'_2)} \times \left(\frac{1}{Q'_2 - Q'_3} \{e^{-Q'_3(t-n)} - e^{-Q'_2(t-n)}\} \right. - \frac{Q'_0 - Q'_2}{(Q'_0 - Q'_1)(Q'_1 - Q'_3)} \{e^{-Q'_3(t-n)} - e^{-Q'_1(t-n)}\} + \left. \frac{Q'_1 - Q'_2}{(Q'_0 - Q'_1)(Q'_0 - Q'_3)} \{e^{-Q'_3(t-n)} - e^{-Q'_0(t-n)}\} \right), \tag{24}$$

where $H(t)$ is the Heaviside step function. The solutions Eqs. (20)–(24) are linear combinations of decaying exponentials with Heaviside functions and are discontinuous at $t = n$. The exponents are related to the outflow rates of each population. We discuss the solutions to the special cases where the outflow rates are equal in Appendix A. We also show that the general case solutions reduce to the special case solutions in the appropriate limit in Appendix A.

Donskoy and Goldschneider (1992) have established that T cell development in the thymus requires input from blood borne precursors throughout postnatal life. This is reflected in the model and the relationships between the parameter values. All of the thymocyte populations are non self-sustaining. That is, any population would decay over time, given that the previous generating population is absent. In the T cell development models of Mehr et al. (1995, 1996), the ranges of parameter values presented could lead to some thymocyte populations being self-sustaining.

Our solutions contrast with Mehr et al. (1995) where logistic growth is used with a carrying capacity placed on all cell populations except DN. Logistic growth is based on the assumption that there is density limiting competition between thymocytes. However, the carrying capacity of the thymus is highly dependent on the stromal cells present as well as thymocytes. Indeed, the development of stromal cells and T cells is intimately linked (Gray et al., 2005; Shortman et al., 1998). Further theoretical studies of this developmental interplay would be valuable. This is beyond the scope of this article. Here we assume that cell populations are well below carrying capacity, hence linear kinetics are appropriate.

The asymptotic behaviour of the solutions is periodic, as we demonstrate below. Consider the function $f(t)$ which is representative of the solutions and let $N = \lfloor t \rfloor$, the largest integer less than or equal to t. Then a representative part of each solution in Eqs. (20)–(24) can be written as

$$f(t) = \sum_{n=0}^{\infty} H(t-n) \exp(-q(t-n)) \tag{25}$$

$$= \exp(-qt) \sum_{n=0}^{N} \exp(nq) \tag{26}$$

$$= \frac{1 - \exp(-q(N+1))}{\exp(q) - 1} \exp[q(1 - \{t - \lfloor t \rfloor\})]. \tag{27}$$

Note that $f(t)$ has discontinuities at integer values of t.

The asymptotic behaviour of $f(t)$ for $t \to \infty$ and hence $N \to \infty$ is

$$f(t) \sim \frac{1}{1 - \exp(-q)} \exp\{-q(t - \lfloor t \rfloor)\}. \tag{28}$$

This is periodic because $t - \lfloor t \rfloor$ is periodic. Also $0 \leqslant t - \lfloor t \rfloor \leqslant 1$. The solutions Eqs. (20)–(24) are simply linear combinations of $f(t)$ with different exponents, hence the asymptotic behaviour of the solutions is periodic with a scaled periodicity of unity. The asymptotic solutions written out explicitly are

$$G_0 \sim \frac{Q_0}{1 - e^{-Q'_0}} e^{-Q'_0(t - \lfloor t \rfloor)}, \tag{29}$$

$$G_1 \sim \frac{Q_0 Q_1}{Q'_0 - Q'_1} \left(\frac{e^{-Q'_1(t-\lfloor t \rfloor)}}{1 - e^{-Q'_1}} - \frac{e^{-Q'_0(t-\lfloor t \rfloor)}}{1 - e^{-Q'_0}} \right), \tag{30}$$

$$G_2 \sim \frac{Q_0 Q_1 Q_2}{Q'_0 - Q'_1} \left(\frac{1}{Q'_1 - Q'_2} \left\{ \frac{e^{-Q'_2(t-\lfloor t \rfloor)}}{1 - e^{-Q'_2}} - \frac{e^{-Q'_1(t-\lfloor t \rfloor)}}{1 - e^{-Q'_1}} \right\} - \frac{1}{Q'_0 - Q'_2} \left\{ \frac{e^{-Q'_2(t-\lfloor t \rfloor)}}{1 - e^{-Q'_2}} - \frac{e^{-Q'_0(t-\lfloor t \rfloor)}}{1 - e^{-Q'_0}} \right\} \right), \tag{31}$$

$$G_3 \sim \frac{Q_0 Q_1 Q_2 Q_3}{(Q'_1 - Q'_2)(Q'_0 - Q'_2)} \times \left(\frac{1}{Q'_2 - Q'_3} \left\{ \frac{e^{-Q'_3(t-\lfloor t \rfloor)}}{1 - e^{-Q'_3}} - \frac{e^{-Q'_2(t-\lfloor t \rfloor)}}{1 - e^{-Q'_2}} \right\} - \frac{Q'_0 - Q'_2}{(Q'_0 - Q'_1)(Q'_1 - Q'_3)} \left\{ \frac{e^{-Q'_3(t-\lfloor t \rfloor)}}{1 - e^{-Q'_3}} - \frac{e^{-Q'_1(t-\lfloor t \rfloor)}}{1 - e^{-Q'_1}} \right\} + \frac{Q'_1 - Q'_2}{(Q'_0 - Q'_1)(Q'_0 - Q'_3)} \left\{ \frac{e^{-Q'_3(t-\lfloor t \rfloor)}}{1 - e^{-Q'_3}} - \frac{e^{-Q'_0(t-\lfloor t \rfloor)}}{1 - e^{-Q'_0}} \right\} \right). \tag{32}$$

The discussion of the periodic behaviour for solutions of the special cases (where $Q'_0 = Q'_1$, $Q'_0 = Q'_2$, etc.) is presented in Appendix A.

For the system to evolve to the mean steady state densities, we balance the inflow and outflow rates of the four populations. Thus,

$$Q_0 = Q'_0, \quad Q_1 = Q'_1, \quad Q_2 = Q'_2, \quad Q_3 = Q'_3. \tag{33}$$

The justification for this is presented in Appendix B. All the parameter values can either be estimated from experimental data or deduced from these relationships. The mean

cell number in the steady state thymus is approximately 1×10^8 with 3% DN, 85% DP and 12% SP. The mean time a cell spends in the N_0 compartment is approximately 3 days, and in the N_2 compartment is 4 days, hence $1/(\lambda_0 + \alpha_{0,1}) = 3$ and $1/(\lambda_2 + \alpha_{2,3}) = 4$. The parameter values are summarised in Table 1.

3. Results

Our model does not consider DN1 explicitly. Its contribution is modelled in the source term for N_0 which represents the DN2 and DN3 cells. We consider a normally distributed source term for N_0 with $4\sigma = 7$ days to model the one week receptivity of the thymic seeding. Note that $8\sigma = T$, hence each seeding distribution is contained well within a period, and that overlaps are effectively zero. Fig. 3 shows that one wave of T cell development appears to cover approximately two seeding cycles, consistent with findings from experimental studies of Foss et al. (2001). Note the sequential appearance of N_0, N_1, N_2 and N_3. The DP population modelled by N_2 is the most numerically dominant.

Table 1
Parameter values were estimated from (Donskoy et al., 2003; Foss et al., 2001; Penit et al., 1995; Shortman et al., 1990; Vasseur et al., 2001) and from private communication with Dr H.T. Petrie. Values of **Q**, β_1, $\alpha_{1,2}$ and κ_3 were deduced from the relationships in Eq. (33). We assume one in three cells receives pre-TCR signalling, hence $\lambda_0 = 2\alpha_{0,1}$, and approximately 5% success in differentiation from N_2 to N_3, hence $\lambda_2 = 20\alpha_{2,3}$

Seeding period, T	28 days
Mean density of N_0, $\tilde{N}_0$	7.5×10^5 cells per thymus
Mean density of N_1, $\tilde{N}_1$	2.25×10^6 cells per thymus
Mean density of N_2, $\tilde{N}_2$	8.5×10^7 cells per thymus
Mean density of N_3, $\tilde{N}_3$	1.2×10^7 cells per thymus
Differentiation rate from N_0 to N_1, $\alpha_{0,1}$	0.11 per day
Death/removal rate of N_0, λ_0	$2\alpha_{0,1}$ per day
Differentiation rate from N_2 to N_3, $\alpha_{2,3}$	0.012 per day
Death/removal rate of N_2, λ_2	20 $\alpha_{2,3}$ per day
Number of cells differentiating to N_0 per seeding, **Q**	7×10^6
Net proliferation rate of N_1, β_1	9.48 per day
Differentiation rate from N_1 to N_2, $\alpha_{1,2}$	9.52 per day
Death/removal rate of N_3, κ_3	0.085 per day

Figs. 4(a) and (b) show the asymptotic temporal profiles of the populations over three seeding cycles, as the steady state thymus covers approximately three cycles. The profiles are periodic and out of phase. The cell numbers in N_0 range from 7×10^3 to 3.1×10^6, in N_1 range from 1.6×10^6 to 2.8×10^6, in N_2 range from 6.7×10^7 to 1.0×10^8 and in N_3 range from 1.1×10^7 to 1.3×10^7. Note the small range of N_3, hence the relatively constant profile. The mean removal of single positives is predicted to be $\kappa_3 \tilde{N}_3 \approx 1 \times 10^6$cells per day, which compares well with standard measurements of T cell production from the thymus (Shortman et al., 1991). The composition of the thymus in terms of percentages is shown in Fig. 4(c) and (d). The total percentage variation of $N_0 + N_1$ is 2–6% which is within the experimentally observed range of percentages for DN cells (excluding the DN1 population). For N_2 the percentage variation is 81–87%, consistent with the observed percentages of DP cells. The N_3 variation is between 10% and 14%.

Cell number variations in steady state thymus composition between mice are generally attributed to intrinsic variations and are often not examined further. This work proposes an alternative explanation that differences may be due to thymii being out-of-phase rather than intrinsic variation alone. Direct experimental confirmation of this is problematic. The standard protocol for cell counting involves sacrificing the animal for thymic harvesting, followed by fluorescent labeling of thymic cell suspension. Cell type is then counted using flow cytometry (Alberts et al., 2002). Therefore, the terminal nature of the procedure precludes obtaining time series data.

Here we propose a mathematical approach to investigate the existence of periodic oscillations in the absence of time series data. Just as a straight line arising from two data sets plotted against one another is indicative of a linear

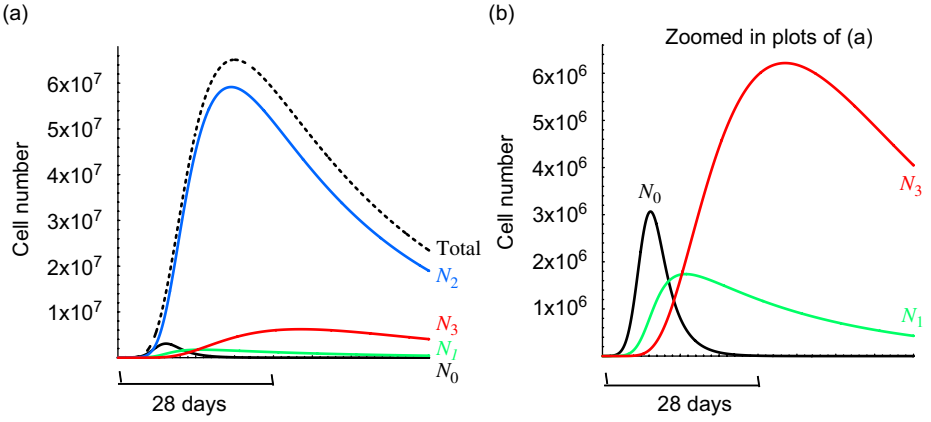

Fig. 3. One cycle of T cell development covers approximately two seeding cycles. The plots are in units of cell number per thymus and days. Parameter values are given in Table 1. (a) Plots of N_0, N_1, N_2, N_3, and the total cell population. (b) Plots of N_0, N_1 and N_3 only.

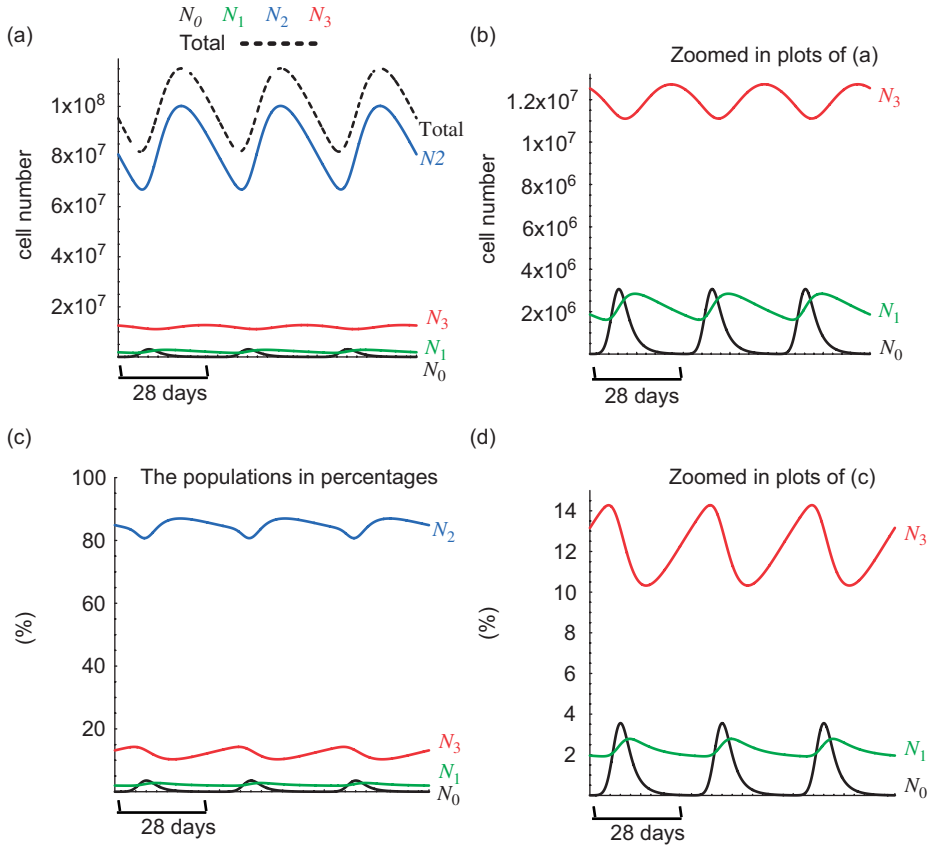

Fig. 4. The asymptotic temporal profiles of the populations over three seeding cycles. The plots are in units of cell number per thymus and days. Parameter values are given in Table 1. (a) Plots of N_0, N_1, N_2, N_3, and the total cell population. (b) Plots of N_0, N_1 and N_3 only. (c) Plots of N_0, N_1, N_2, N_3 expressed as a percentage of the total population. (d) Percentage plots of N_0, N_1 and N_3 only.

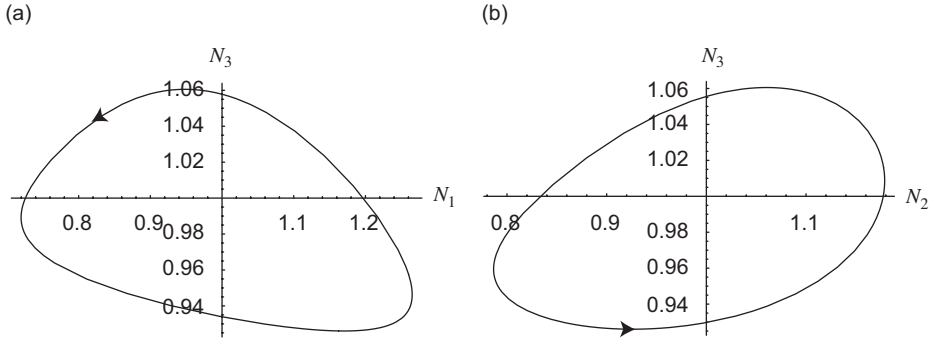

Fig. 5. Phase plane of cell number. The plots are in dimensionless units. The arrow heads indicate the direction of time. Periodic behaviour produces closed loops when populations are plotted against each other. For example (a) N_1 versus N_3 and (b) N_2 versus N_3.

relationship, a closed plot of two out-of-phase cell populations with the same periodicity is indicative of periodic oscillations. After sampling the cell numbers from a large number of steady state thymii, the cell numbers of two populations can be plotted against each other to test this model, as illustrated in Fig. 5. We note that in order to validate periodic fluctuations in this way, the intrinsic variation between animal thymii must be significantly less than the variation due to being out-of-phase.

Fitting the model to experimental data can provide the parameter values $\bar{\sigma}$, Q_0, Q_0', Q_1, Q_1', Q_2, Q_2', Q_3, and Q_3'. We assumed that the inflow and outflow rates of all populations are balanced giving the relationships in Eq. (33), so the actual number of parameter values is only five. The functions for fitting are $N_0(t;\bar{\sigma},Q_0)$, $N_1(t;\bar{\sigma},Q_0,Q_1)$, $N_2(t;\bar{\sigma},Q_0,Q_1,Q_2)$ and $N_3(t;\bar{\sigma},Q_0,Q_1,Q_2,Q_3)$. This may appear to be a large number of parameter values; however, four populations give six different combinations. The parameter values $\bar{\sigma},Q_0,Q_1$ can be obtained from all six combinations, Q_2 from five combinations and Q_3 from three combinations. The large number of combinations in estimating each parameter value restrict the degree of

freedom and serve as a consistency check. The most useful parameter value to be obtained is $\bar{\sigma}$. It provides a measure of the discreteness of seeding or the relative receptivity time of the thymus to the seeding period. This is roughly quantified by experiments to be one week over four weeks. The other parameter values are measures of the scaled inflow and outflow rates of each population.

Here we outline how curve fitting can proceed after obtaining experimental data. The task is to fit two functions of the form $x(t;p_1,p_2,\ldots p_n)$ and $y(t;p_1,p_2,\ldots p_n)$ to a set of data $\{x_i,y_i\}$ to extract the parameter values $p_1,p_2,\ldots p_n$. It is not immediately obvious how residuals should be calculated as we are fitting a parametric curve $\mathbf{r}(t)=(x(t),y(t))$ to a set of data points that do not have time information. The missing time information corresponding to a point on the curve needs to be calculated. We show graphically how the residuals are calculated in Fig. 6. For every data point (x,y), marked by red dots on Fig. 6, we look for a corresponding point $(x(t'),y(t'))$ marked by black dots on the curve such that the line between the two is perpendicular to the tangent. The residual is measured by the length of this line. The tangent vector is simply $\mathbf{r}'(t)$. Parameter values can then be extracted by using an optimisation technique to minimise the residuals. Statistical analysis of residuals can be used to suggest refinements to the current model.

3.1. Sensitivity to parameter values

We simulated the steady state thymus using parameter values that give mean values of unity for all populations. This is discussed in Appendix B. For ease of comparison, we consider the effect of changing one parameter value at a time and use the superscript 'new' while keeping the previously estimated parameter values fixed. Consider varying the seeding period so that $T^{\text{new}}/T=a$ for $a\neq 1$. It is straight forward to see from our definitions in Eqs. (9)–(12) that the mean values of all populations will be affected by a factor of $1/a$. If the number of cells differentiating to N_0 per seeding period is varied so that $\mathbf{Q}^{\text{new}}/\mathbf{Q}=a$, then the mean values of all populations are affected by a factor of a.

Varying the differentiation parameter values affects the mean population values in the following way. For example, consider $\alpha_{0,1}^{\text{new}}/\alpha_{0,1}=a$ so that

$$Q_0'^{\text{new}}=T(a\alpha_{0,1}+\lambda_0), \tag{34}$$

and

$$Q_1^{\text{new}}=\frac{Ta\alpha_{0,1}\tilde{N}_0}{\tilde{N}_1}. \tag{35}$$

Recall that balancing the inflow and outflow rates of N_0 gives us the relation $\mathbf{Q}/\tilde{N}_0=T(\alpha_{0,1}+\lambda_0)$. The mean value of N_0 is

$$\langle G_0^{\text{new}}\rangle=\frac{Q_0}{Q_0'^{\text{new}}}=\frac{\mathbf{Q}}{\tilde{N}_0}\frac{1}{T(a\alpha_{0,1}+\lambda_0)}, \tag{36}$$

$$=\frac{1}{a+c(1-a)}, \tag{37}$$

where

$$c=\frac{\lambda_0}{\alpha_{0,1}+\lambda_0}. \tag{38}$$

This is a monotonically decreasing function of a, which is expected as the mean value of N_0 would decrease with increasing differentiation rate to N_1.

The subsequent populations N_1, N_2, N_3 are affected by a extra factor of a due to Q_1^{new}, hence

$$\langle G_1^{\text{new}}\rangle=\langle G_2^{\text{new}}\rangle=\langle G_3^{\text{new}}\rangle=\frac{a}{a+c(1-a)}. \tag{39}$$

This is a monotonically increasing function of a. The mean values of these populations are expected to increase with increasing differentiation rate from N_0 to N_1.

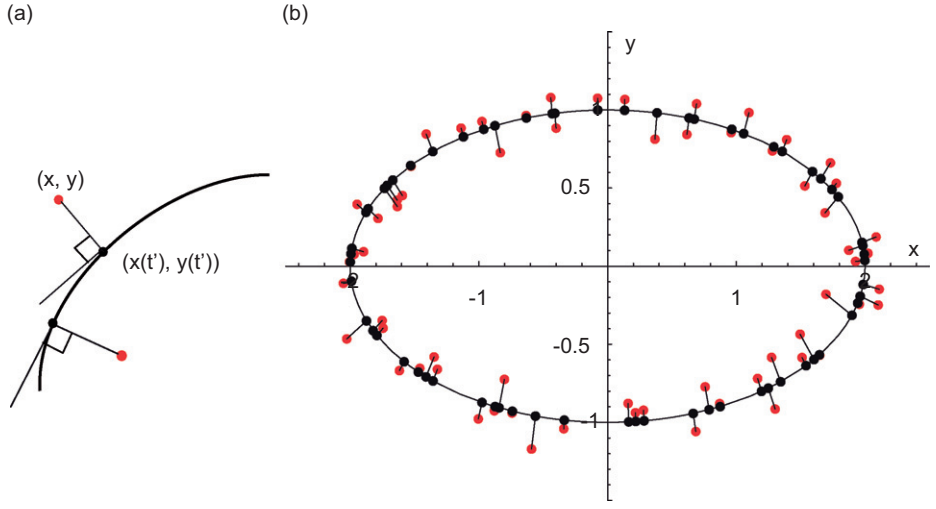

Fig. 6. An example of fitting a parametric curve, an ellipse, $\mathbf{r}(t)=(a\cos(t),b\sin(t))$ to data. The parameter values are $a=2$, $b=1$. The residuals are indicated by the line joining data points, in red, and the corresponding points on the curve, in black.

Similar analysis applies to the other parameter values. These relationships allow adjustments to the estimated parameter values in light of more accurate measurements from experiments. One can also use the relationships to postulate the relevant parameter values responsible for perturbed mean densities of thymocyte populations, under pathological conditions for example.

4. Conclusion

The periodic seeding of progenitor cells to the steady state thymus raises questions of how the relatively constant number of cells in the thymus are maintained and how relatively constant number of T cells are produced. Using a simple model with linear kinetics, our results verify the synchronous wave development hypothesis of Goldschneider and co-workers (Donskoy et al., 2003; Foss et al., 2001; Goldschneider, 2006). The alternative asynchronous release hypothesis of Petrie and co-workers (Porritt et al., 2003) would also allow constant output of T cells. Asynchronous release would operate independently of the DN1 population to let a constant number of cells differentiating to DN2 over time. This is equivalent to considering that the source term of N_0 (in reference to Eq. (1)) is constant for all time, hence $S(t) = 1/T$ and all populations would be constant. We have shown that the production of T cells can appear relatively constant without assuming asynchronous release mechanisms.

Our results show periodic out-of-phase behaviour of the thymocyte populations. It may be surprising to find periodic oscillations in what is generally regarded as a steady state thymus. However, oscillations are common in the immune system (Stark et al., 2007). We propose experiments to sample the steady thymus which will construct a phase plane of thymocyte populations. Experimental data can then be used to support or refute the synchronous development hypothesis of T cells and the existence of periodic oscillations in the thymus.

Recently, Mehr (2006) has highlighted the importance of understanding the underlying mechanisms of feedback loops and nonlinearities in the immune system. In the current model we have assumed linear kinetics in T cell development. However, there is some suggestion that nonlinearities may exist at the DP stage, during positive selection. DP cells have a relatively short life span and outnumber stromal cells by approximately one hundred orders of magnitude (Gray et al., 2006). Therefore, it is reasonable to propose that nonlinearities can arise due to this competition for critical signals needed for survival and differentiation (Fink, 2003). Understanding the dynamics of positive selection will provide insight into this stringent step of development where only an estimated 3–5% of DPs are successful.

The co-ordinated mobilisation of progenitor cells from the bone marrow and the opening of niches in the thymus (Donskoy et al., 2003) strongly suggest thymus-bone marrow feedback mechanisms. Numerous components of this feedback mechanism are reviewed by Goldschneider (2006). Extensions to the current model of thymopoiesis could involve feedbacks and time delays. Analogies to this control mechanism might be found in models of haematopoiesis (Mackey and Glass, 1977), where bifurcation from periodic to chaotic solutions was shown. Hence, there may exist more complicated dynamics in the thymus than previously assumed.

The understanding of T cell developmental processes has widespread implications in many health-related situations. Further experimental investigations guided by theoretical approaches are warranted (Chakraborty et al., 2003; Witt et al., 2005b).

Acknowledgements

A.Q. Cai, K.A. Landman, and B.D. Hughes are supported by the Particulate Fluids Processing Centre, an Australian Research Council (ARC) Special Research Centre at the University of Melbourne, and the ARC Discovery Grant Scheme. A.Q. Cai is supported by an Australian Postgraduate Award and a Postgraduate Overseas Research Experience Scholarship. C. M. Witt is supported by NIH/NCRR grant number 5G12RR013646. A.Q. Cai wishes to thank Dr Richard Schugart and Professor Avner Friedman from the Mathematical Biosciences Institute at Ohio State University for helpful discussions. C.M. Witt wishes to thank Dr H.T. Petrie for helpful discussions. The authors also wish to thank Dr Ray Watson.

Appendix A. The special case

The results of Eqs. (20)–(24) make use of the following differential equations and their solutions:

$$\frac{\mathrm{d}\mathbf{F}}{\mathrm{d}t} + B\mathbf{F} = \delta_+(t-n), \quad \mathbf{F}(0) = 0, \tag{A.1}$$

$$\mathbf{F} = H(t-n)\,\mathrm{e}^{-B(t-n)}, \tag{A.2}$$

and

$$\frac{\mathrm{d}\mathbf{f}}{\mathrm{d}t} + A\mathbf{f} = H(t-n)\mathrm{e}^{-B(t-n)}, \quad \mathbf{f}(0) = 0, \tag{A.3}$$

$$\mathbf{f} = \begin{cases} H(t-n)\dfrac{1}{B-A}\{\mathrm{e}^{-A(t-n)} - \mathrm{e}^{-B(t-n)}\}, & \text{if } A \neq B, \\ H(t-n)(t-n)\mathrm{e}^{-A(t-n)}, & \text{if } A = B, \end{cases} \tag{A.4}$$

where A and B are constants.

For the special case where $Q_0' = Q_1'$, $Q_0' = Q_2'$, etc., the solutions to the system Eqs. (16)–(19) have a representative function

$$g(t) = \sum_{n=0}^{\infty} H(t-n)(t-n)\exp(-q(t-n)), \tag{A.5}$$

$$= -\frac{\mathrm{d}}{\mathrm{d}q} f(t), \tag{A.6}$$

where $f(t)$ is defined in Eq. (28). In the main text, we showed that $f(t)$ is asymptotically periodic. Hence the asymptotic behaviour of $g(t)$ is also periodic.

The general solution for $A \neq B$ reduces to the special case solution for $A = B$ if we take the limit $A - B \to 0$. Consider

$$s(t) = \frac{1}{B-A}(e^{-At} - e^{-Bt})$$
$$= \frac{1}{B-A}\sum_{n=1}^{\infty}\frac{(-t)^n}{n!}(A^n - B^n) \quad (A.7)$$
$$= \frac{1}{B-A}\sum_{n=1}^{\infty}\frac{(-t)^n}{n!}(A-B)\sum_{j=0}^{n-1}A^j B^{n-1-j} \quad (A.8)$$
$$\to t\sum_{n=1}^{\infty}\frac{(-t)^{n-1}}{(n-1)!}A^{n-1} = te^{-At}. \quad (A.9)$$

Appendix B. The relationship between parameter values

We define the mean steady state values as

$$\langle G_i\rangle = \lim_{M\to\infty}\int_M^{M+1} G_i\,dt, \quad i = 0,1,2,3. \quad (B.1)$$

The system Eqs. (16)–(19) approaches an asymptotic periodic state, thus

$$\int_M^{M+1}\frac{dG_i}{dt}\,dt \to 0, \quad i = 0,1,2,3. \quad (B.2)$$

The system of Eqs. (16)–(19) becomes

$$0 = Q_0 - Q_0'\langle G_0\rangle, \quad (B.3)$$
$$0 = Q_1\langle G_0\rangle - Q_1'\langle G_1\rangle, \quad (B.4)$$
$$0 = Q_2\langle G_1\rangle - Q_2'\langle G_2\rangle, \quad (B.5)$$
$$0 = Q_3\langle G_2\rangle - Q_3'\langle G_3\rangle. \quad (B.6)$$

The Eqs. (B.3)–(B.6) can be rewritten as

$$\langle G_0\rangle = \frac{Q_0}{Q_0'}, \quad \langle G_1\rangle = \frac{Q_1}{Q_1'}\langle G_0\rangle,$$
$$\langle G_2\rangle = \frac{Q_2}{Q_2'}\langle G_1\rangle, \quad \langle G_3\rangle = \frac{Q_3}{Q_3'}\langle G_2\rangle. \quad (B.7)$$

For the system to evolve to the mean steady state densities, we require

$$\langle G_i\rangle = 1, \quad i = 0,1,2,3. \quad (B.8)$$

Hence, Eqs. (B.7) and (B.8) produce the balance of parameter values given in Eq. (33).

References

Alberts, B., Johnson, A., Lewis, J., Raff, M., Roberts, K., Walter, P., 2002. Molecular Biology of the Cell, fourth ed. Garland Science, Taylor and Francis Group.

Chakraborty, A.K., Dustin, M.L., Shaw, A.S., 2003. In silico models for cellular and molecular immunology: successes, promises, and challenges. Nat. Immunol. 4, 933–936.

Donskoy, E., Goldschneider, I., 1992. Thymocytopoiesis is maintained by blood-borne precursors throughout postnatal life. A study in parabiotic mice. J. Immunol. 148, 1604–1612.

Donskoy, E., Foss, D., Goldschneider, I., 2003. Gated importation of prothymocytes by adult mouse thymus is coordinated with their periodic mobilization from bone marrow. J. Immunol. 171, 3568–3575.

Efroni, S., Harel, D., Cohen, I.R., 2007. Emergent dynamics of thymocyte development and lineage determination. PLoS Comput. Biol. 3, 0127–0136.

Egerton, M., Shortman, K., Scollay, R., 1990. The kinetics of immature murine thymocyte development in vivo. Int. Immunol. 2 (6), 501–507.

Fink, P.J., 2003. Deadbeat neighbors influence thymocyte lineage commitment. Nat. Immunol. 5, 727–728.

Foss, D.L., Donskoy, E., Goldschneider, I., 2001. The importation of hematogenous precursors by the thymus in a gated phenomenon in normal adult mice. J. Exp. Med. 193, 365–374.

Goldschneider, I., 2006. Cyclical mobilization and gated importation of thymocyte progenitors in the adult mouse: evidence for a thymus-bone marrow feedback loop. Immunol. Rev. 209, 58–75.

Gray, D.H.D., Ueno, T., Chidgey, A.P., Malin, M., Goldberg, G.L., Takahama, Y., Boyd, R.L., 2005. Controlling the thymic microenvironment. Curr. Opin. Immunol. 17, 137–143.

Gray, D.H.D., Seach, N., Ueno, T., Milton, M.K., Liston, A., Lew, A.M., Goodnow, C.C., Boyd, R.L., 2006. Developmental kinetics, turnover, and stimulatory capacity of thymic epithelial cells. Blood 108, 3777–3785.

Lind, E.F., Prockop, S.E., Porritt, H.E., Petrie, H.T., 2001. Mapping precursor movement through the postnatal thymus reveals specific microenvironments supporting defined stages of early lymphoid development. J. Exp. Med. 194, 127–134.

Mackey, M.C., Glass, L., 1977. Oscillation and chaos in physiological control systems. Science 197 (4300), 287–289.

Mehr, R., 2006. Feedback loops, reversals and nonlinearities in lymphocyte development. Bull. Math. Biol. 68, 1073–1094.

Mehr, R., Globerson, A., Perelson, A.S., 1995. Modeling positive and negative selection and differentiation processes in the thymus. J. Theor. Biol. 175, 103–126.

Mehr, R., Perelson, A.S., Fridkis-Hareli, M., Globerson, A., 1996. Feedback regulation of t cell development in the thymus. J. Theor. Biol. 181, 157–167.

Penit, C., Lucas, B., Vasseur, F., 1995. Cell expansion and growth arrest phases during the transition from precursor (CD4-8-) to immature (CD4 + 8+) thymocytes in normal and genetically modified mice. J. Immunol. 154, 5103–5113.

Petrie, H.T., Zúñiga-Pflücker, J.C., 2007. Zoned out: functional mapping of stromal signaling microenvironments in the thymus. Annu. Rev. Immunol. 25, 649–679.

Porritt, H.E., Gordon, K., Petrie, H.T., 2003. Kinetics of steady-state differentiation and mapping of intrathymic-signaling environments by stem cell transplantation in nonirradiated mice. J. Exp. Med. 198, 957–962.

Shi, H., Ma, W., 2006. An improved model of t cell development in the thymus and its stability analysis. Math. Biosci. Eng. 3, 237–248.

Shortman, K., Egerton, M., Spangrude, G.J., Scollay, R., 1990. The generation and fate of thymocytes. Sem. Immunol. 2, 3–12.

Shortman, K., Vremec, D., Egerton, M., 1991. The kinetics of t cell antigent receptor expression by subgroups of $cd4 + 8+$ thymocytes: delineation of $cd4 + 8 + 3^{2+}$ thymocytes as post-selection intermediates leading to mature cells. J. Exp. Med. 173, 323–332.

Shortman, K., Vremec, D., Corcoran, L.M., Georgopoulos, K., Lucas, K., Wu, L., 1998. The linkage between t-cell and dendritic cell development in the mouse thymus. Immunol. Rev. 165, 39–46.

Stark, J., Chan, C., George, A.J.T., 2007. Oscillations in the immune system. Immunol. Rev. 216, 213–231.

Vasseur, F., Campion, A.L., Penit, C., 2001. Scheduled kinetics of cell proliferation and phenotypic changes during immature thymocyte generation. Eur. J. Immunol. 31, 3038–3047.

Wang, G., 2007. Estimation of the proliferation and maturation functions in a physiologically structured model of thymocyte development. J. Math. Biol. 54, 761–786.

Wang, G., Krueger, G.R.F., 2004. A general mathematical method for investigating the thymic microenvironment, thymocyte development, and immunopathogenesis. Math. Biosci. Eng. 1, 289–305.

Witt, C.M., Robey, E.A., 2005. Thymopoiesis in 4 dimensions. Sem. Immunol. 17, 95–102.

Witt, C.M., Raychaudhur, S., Schaefer, B., Chakraborty, A.K., Robey, E.A., 2005a. Directed migration of positively selected thymocytes visualized in real time. PLoS Biol. 3, 0001–0008.

Witt, C.M., Raychaudhuri, S., Chakraborty, A.K., 2005b. Movies, measurement, and modeling: the three Ms of mechanistic immunology. J. Exp. Med., commentary 201, 501–504.

Ye, P., Kirschner, D.E., 2002. Reevaluation of T cell receptor excision circles as a measure of human recent thymic emigrants. J. Immunol. 169, 4968–4979.